



Supplement of

Changes in water quality and ecosystem processes at extreme summer low flow of 2018 with high-frequency sensors

Jingshui Huang et al.

Correspondence to: Jingshui Huang (jingshui.huang@tum.de)

The copyright of individual parts of the supplement might differ from the article licence.

1 **S1. Phytoplankton Growth Rate and Temperature Dependence**

2 The net growth rate term G_p for the phytoplankton from our previous model was dynamically calculated
3 as:

$$G_p = k_G - k_R - k_D \quad (S1)$$

4 where k_G is the temperature-dependent growth rate, and k_R , k_D represent respiration and death rates,
5 respectively.

6 The phytoplankton growth rate k_G is given by:

$$k_G = k_{Gmax} \times X_T \times X_L \times X_N \quad (S2)$$

7 with the components defined as follows:

- 8 • k_{Gmax} : Maximum growth rate at 20°C, day⁻¹ (0.5-4.0)
- 9 • X_T : Temperature multiplier
- 10 • X_L , X_N : Light and nutrient limitation factors (dimensionless, range 0–1)

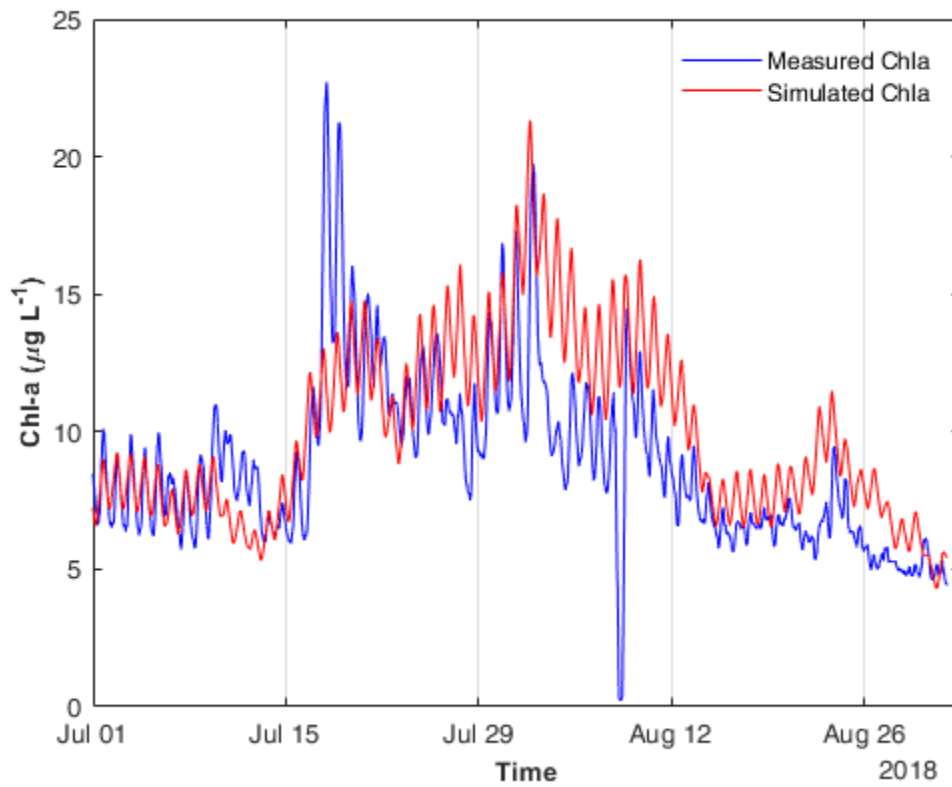
11 The temperature multiplier X_T was calculated using an asymmetric Gaussian response function:

$$X_T = \begin{cases} \exp[-\kappa_1(T_{opt}-T)^2] & \text{if } T \leq T_{opt} \\ \exp[-\kappa_2(T-T_{opt})^2] & \text{if } T > T_{opt} \end{cases} \quad (S3)$$

14 where:

- 15 • T_{opt} : Optimum temperature for growth, 10–27 °C (set to 13 °C in this study)
- 16 • κ_1 , κ_2 : Temperature sensitivity coefficients below and above T_{opt} (both set to 0.02 °C⁻²)

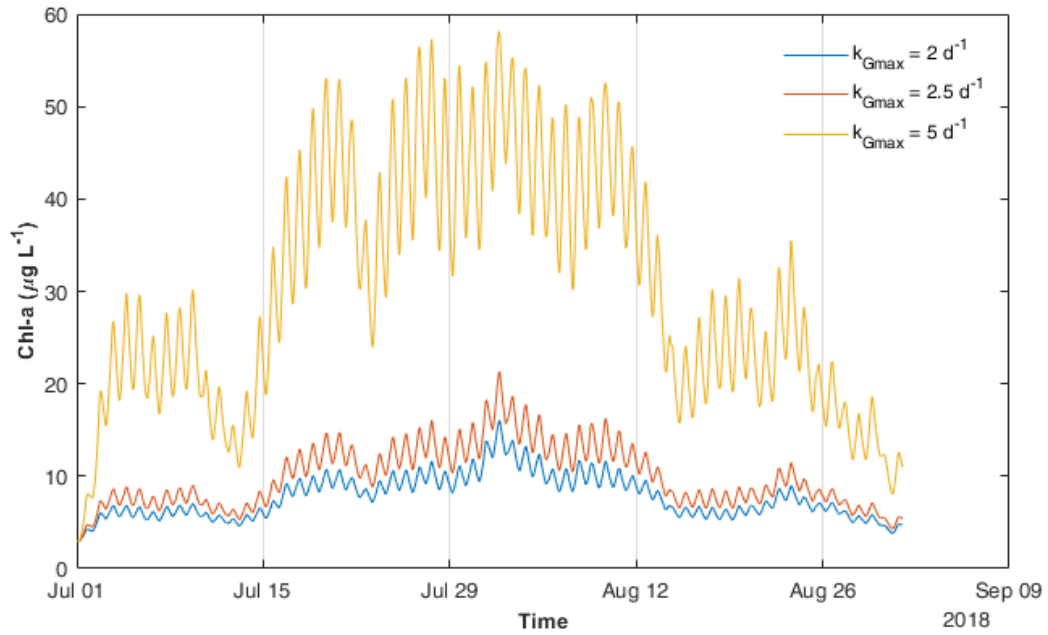
17 This formulation captures the decline in growth at supraoptimal temperatures and reflects the thermal
18 preferences of diatom-dominated phytoplankton typical of the Lower Bode.



20

21 **Fig. S1** Measured and simulated Chl a concentration in the ExLF period at the STF station.

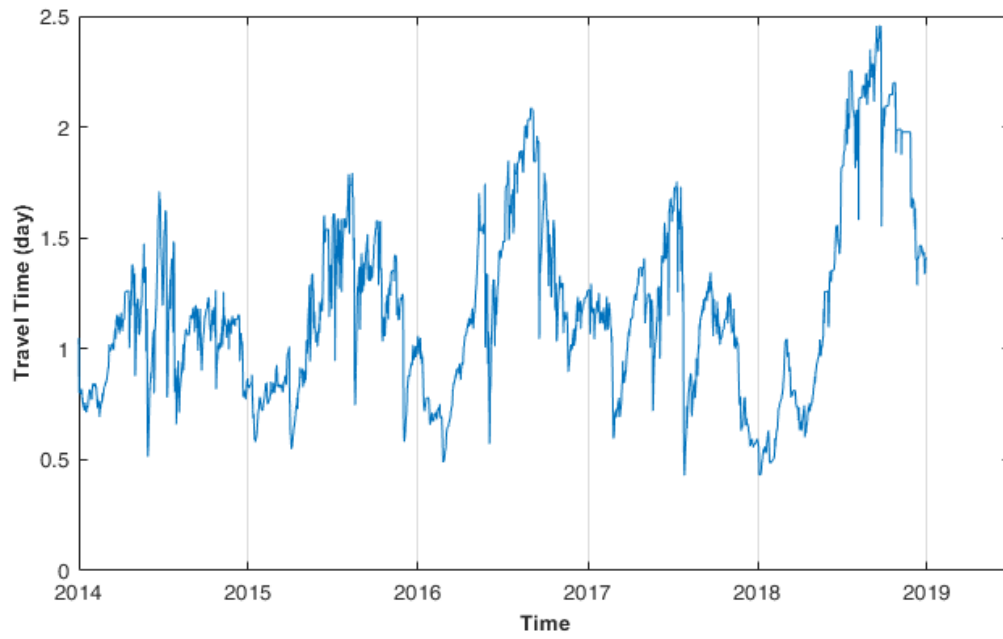
22



23

24 **Fig. S2** Simulated Chl *a* concentrations in the ExLF period at STF with different values of
 25 phytoplankton maximum growth rate constant at 20°C (k_{Gmax}) applied to the water quality model in
 26 Huang et al. (2022). The optimal value for k_{Gmax} is 2.5 d^{-1} in the original model set-up in Huang et al.
 27 (2022). With the changing k_{Gmax} values, both the overall Chl *a* concentrations and the diurnal delta of
 28 the concentration changed accordingly.

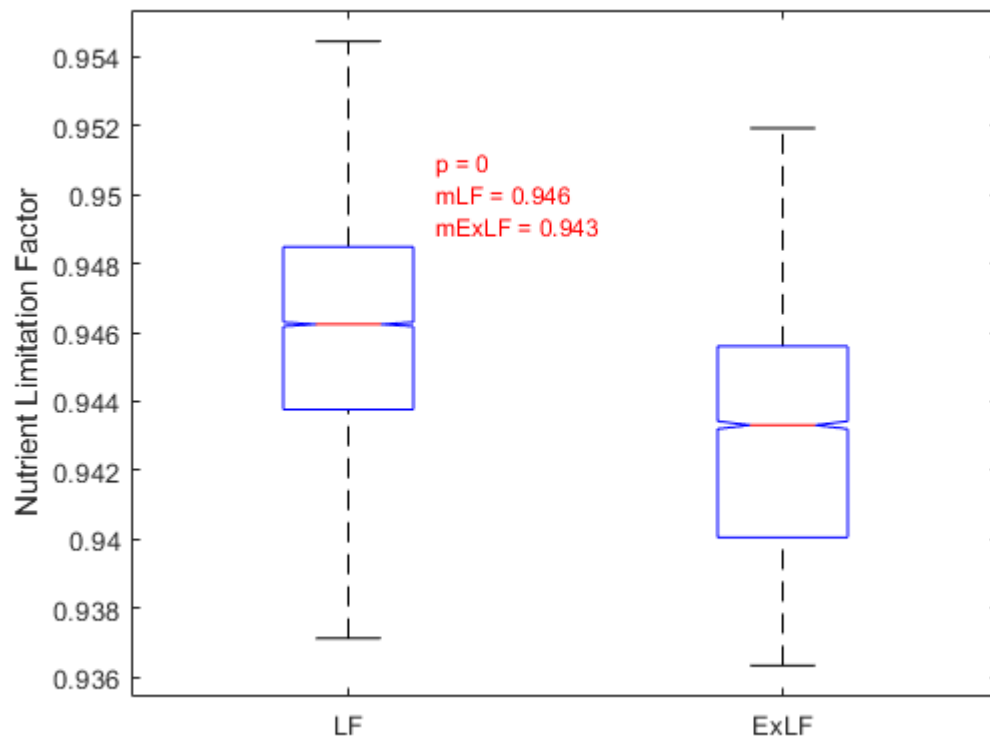
29



30

31 **Fig. S3** Water travel time from GGL to STF in the Lower Bode reach in 2014-2018.

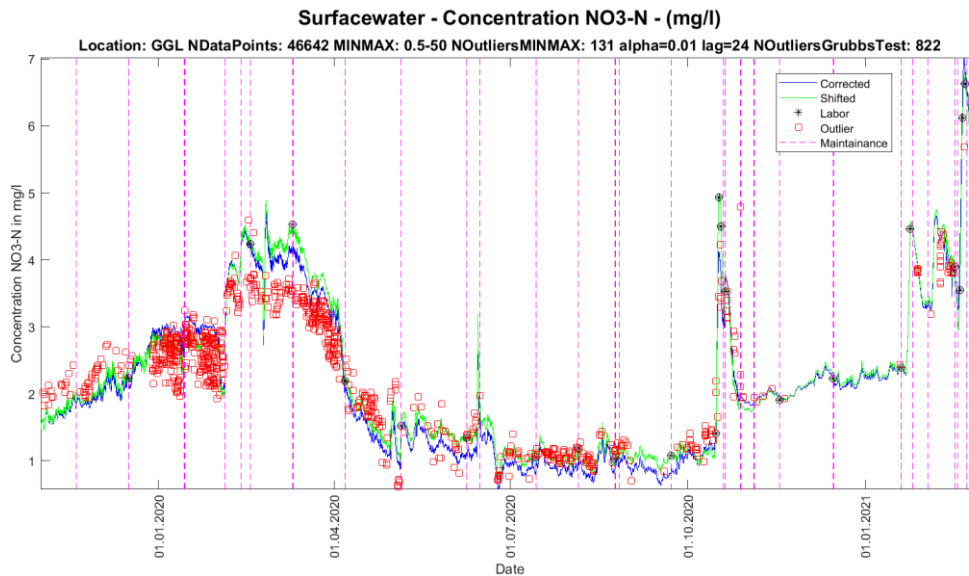
32



33

34 **Fig. S4** Nutrient limitation (range: 0-1) calculated in WASP during LF and ExLF periods.

35



36

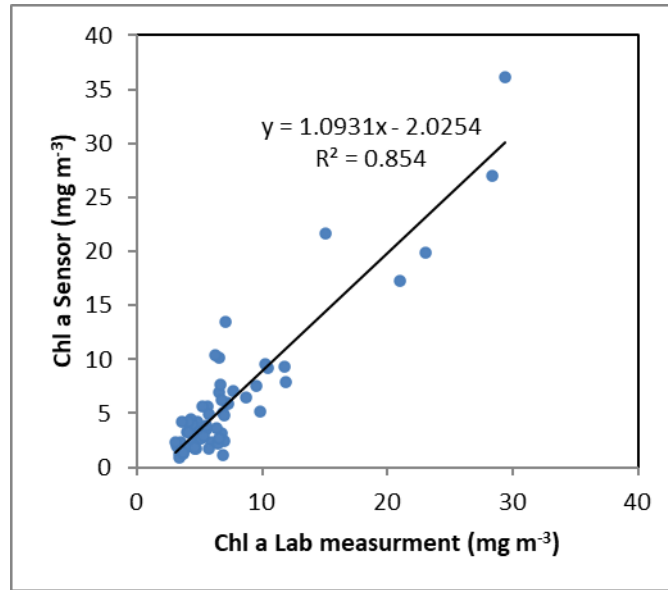
37 **Fig. S5** Comparison of nitrate (NO_3^- -N) concentrations measured by sensor and laboratory analyses,
 38 including data adjustments at the GGL station.

39 For NO_3^- , we compared sensor readings with laboratory-analyzed grab samples and applied corrections
 40 following the established methodology of Rode et al. (2016) from the Bode observatory in the Selke
 41 River. In that study, the method achieved an R^2 of 0.93 with low bias at Station Meisdorf. In our case,
 42 we also provide a comparison of sensor and laboratory measurements, together with the corrected NO_3^-
 43 data for the GGL station in Fig. S5, which demonstrates the good agreement between the original sensor
 44 measurements and the grab samples, with only minor bias.

45 Sensor data were corrected against grab samples using our automated MATLAB data-cleaning tool,
 46 which shifts the continuous sensor signal to align with laboratory results when necessary. This step is
 47 particularly important for NO_3^- because of the characteristics of the UV-Vis absorbance method: the
 48 optical path length is fixed during measurements, while the optimal path length depends on
 49 concentration (e.g., ~ 1 cm for low concentrations and ~ 0.2 cm for high concentrations). When
 50 concentrations vary strongly, measurement uncertainties may occur if the path length remains constant.
 51 Corrections against laboratory data are therefore especially relevant during rare periods of elevated
 52 NO_3^- concentrations. We apply this correction only to nitrate for the above methodological reason, and
 53 an example of this adjustment is shown in Fig. S5 for the GGL Station.

54

55



56

57 **Fig. S6** Relationship between *Chl-a* concentrations measured by sensors and laboratory grab samples
58 at the STF station from 2011 to 2019.

59

60

61

62 **Table S1** Summary of 5th, 25th, 50th, 75th, and 95th Percentile Values and Statistical Comparison Between
 63 LF and ExLF Conditions for Key Water Quality and Metabolic Variables.

64 **Abbreviations:** Q – discharge (m³ s⁻¹); WT – water temperature (°C); NO₃⁻ – nitrate concentration (mg N L⁻¹); DO –
 65 dissolved oxygen (mg L⁻¹); DO_{max} / DO_{min} – daily maximum/minimum DO; DO_Δ – daily DO range (DO_{max} – DO_{min}); DO_s
 66 – DO saturation concentration; DO_D – DO deficit (DO_s – DO); Chl *a* – chlorophyll *a* concentration (μg L⁻¹); Chl *a*_{max} /
 67 Chl *a*_{min} – daily maximum/minimum Chl *a*; Chl *a*_Δ – daily Chl *a* range; GPP – gross primary production (g O₂ m⁻² d⁻¹);
 68 ER – ecosystem respiration (g O₂ m⁻² d⁻¹); NEP – net ecosystem production (GPP – ER); GPP:ER – ratio of gross
 69 primary production to respiration; GPP_{Phy} – phytoplankton-based GPP; GPP_{Ben} – benthic algae-based GPP; U_{net-NO₃⁻}
 70 – net nitrate uptake rate (mg N m⁻² d⁻¹); Perc_{net-NO₃⁻} – percentage of nitrate uptake over the reach; t_T – water
 71 travel time (days); Solar radiation – incoming solar radiation (Langley per day).

Variable	LF_5	LF_25	LF_50	LF_75	LF_95	ExLF_5	ExLF_25	ExLF_50	ExLF_75	ExLF_95
Q_GGL	2.66	3.27	3.86	4.45	5.72	2.27	2.38	2.48	2.75	3.17
Q_STF	2.85	3.36	3.81	4.60	5.73	2.05	2.17	2.47	2.84	3.42
WT_GGL	16.17	17.56	19.07	20.56	22.16	16.06	18.07	19.49	21.33	23.51
WT_STF	18.26	19.50	21.13	22.75	24.57	18.84	20.74	22.02	23.96	25.82
NO ₃ ⁻ _GGL	1.22	1.44	1.61	1.78	2.19	1.36	1.46	1.55	1.66	1.85
NO ₃ ⁻ _STF	1.15	1.38	1.58	1.71	2.12	1.29	1.37	1.43	1.52	1.67
t _T	1.28	1.48	1.62	1.78	2.02	1.82	1.99	2.12	2.19	2.25
Solar Radiation	0.00	0.00	41.73	197.87	344.59	0.00	0.00	41.73	218.06	376.90
DO_GGL	7.08	8.01	8.75	9.66	10.88	6.42	7.49	8.45	9.68	10.81
DO_STF	7.21	8.00	8.50	8.98	9.64	6.50	7.35	8.04	8.75	9.58
DO _{max} _GGL	8.22	9.29	10.00	10.72	11.71	9.24	9.83	10.45	10.89	11.57
DO _{max} _STF	7.75	8.51	9.04	9.46	10.09	7.32	8.60	9.32	9.61	10.06
DO _{min} _GGL	6.45	7.22	7.72	8.11	8.67	5.91	6.42	7.01	7.43	7.77
DO _{min} _STF	6.52	7.36	7.90	8.31	8.89	5.84	6.57	7.17	7.78	8.13
DO _Δ _GGL	0.91	1.68	2.36	3.11	3.58	2.53	3.08	3.54	3.81	4.44
DO _Δ _STF	0.43	0.80	1.05	1.42	2.31	1.11	1.62	1.78	2.39	2.79
DO _D _GGL	-0.29	0.10	0.48	0.89	1.57	0.18	0.27	0.60	0.90	1.27
DO _D _STF	-0.26	0.19	0.49	0.74	1.50	-0.09	0.34	0.64	1.03	1.66
Chl <i>a</i> _GGL	2.72	3.08	3.93	4.82	6.49	2.84	3.20	3.62	4.22	5.40
Chl <i>a</i> _STF	4.32	5.60	6.65	8.40	11.89	5.04	6.56	8.27	10.61	14.51
Chl <i>a</i> _{max} _GGL	2.82	3.47	4.67	5.82	9.36	3.01	3.56	4.47	5.11	6.11
Chl <i>a</i> _{max} _STF	4.65	6.12	7.60	9.93	14.47	5.62	7.59	9.87	12.93	19.87
Chl <i>a</i> _{min} _GGL	2.58	2.89	3.73	4.61	6.00	2.64	2.87	3.28	3.56	4.28
Chl <i>a</i> _{min} _STF	3.72	4.91	6.05	7.12	9.41	4.66	5.87	6.63	9.05	11.36
Chl <i>a</i> _Δ _GGL	0.07	0.44	0.65	1.18	3.81	0.32	0.71	1.14	1.51	2.55
Chl <i>a</i> _Δ _STF	0.54	0.98	1.63	2.92	6.15	0.79	1.51	2.82	4.10	9.49
GPP	0.68	1.34	1.83	2.28	2.86	1.58	2.21	2.67	2.88	3.16
ER	1.47	2.02	2.48	2.91	4.17	2.30	2.66	3.05	3.40	3.82
NEP	-2.70	-1.15	-0.55	-0.10	0.34	-1.23	-0.70	-0.46	-0.21	-0.11
GPP:ER	0.24	0.54	0.80	0.95	1.18	0.58	0.76	0.84	0.92	0.96
GPP _{Phy}	0.12	0.25	0.38	0.61	0.93	0.08	0.30	0.46	0.65	0.89
GPP _{Ben}	0.21	0.83	1.31	1.98	2.37	1.24	1.81	2.07	2.37	2.72
U _{NET-NO₃⁻}	-95.64	15.79	99.79	211.58	832.56	-18.03	46.72	101.07	153.89	218.12
Perc _{NET-NO₃⁻}	-0.05	0.02	0.07	0.13	0.26	-0.01	0.06	0.12	0.19	0.29

73 **References**

74 Huang, J., Borchardt, D., and Rode, M.: How do inorganic nitrogen processing pathways
75 change quantitatively at daily, seasonal, and multiannual scales in a large agricultural stream?,
76 Hydrol. Earth Syst. Sci., 26, 5817-5833, 10.5194/hess-26-5817-2022, 2022.

77 Rode, M., Halbedel née Angelstein, S., Anis, M. R., Borchardt, D., and Weitere, M.:
78 Continuous In-Stream Assimilatory Nitrate Uptake from High-Frequency Sensor
79 Measurements, Environmental Science & Technology, 50, 5685-5694,
80 10.1021/acs.est.6b00943, 2016.

81